

Host–Guest Behavior of a Heavy-Atom Heterocycle $\text{Re}_4(\text{CO})_{16}(\mu\text{-SbPh}_2)_2(\mu\text{-H})_2$ Obtained from a Palladium-Assisted Ring Opening Dimerization of $\text{Re}_2(\text{CO})_8(\mu\text{-SbPh}_2)(\mu\text{-H})$

Richard D. Adams,* William C. Pearl, Jr., and Yuen Onn Wong

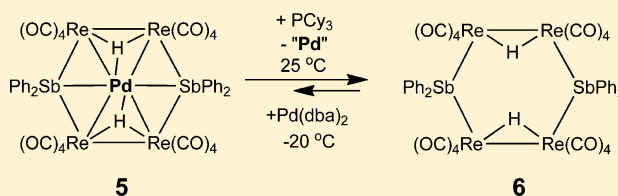
Department of Chemistry and Biochemistry, University of South Carolina, Columbia, South Carolina 29208, United States

Michael B. Hall* and Justin R. Walensky

Department of Chemistry, Texas A&M University, College Station, Texas 77843, United States

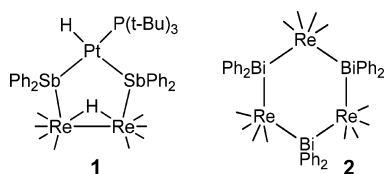
Supporting Information

ABSTRACT: The heavy-atom heterocycle $\text{Pd}[\text{Re}_2(\text{CO})_8(\mu\text{-SbPh}_2)(\mu\text{-H})]_2$ (**5**) has been synthesized by the palladium-catalyzed ring-opening cyclodimerization of the three-membered heterocycle $\text{Re}_2(\text{CO})_8(\mu\text{-SbPh}_2)(\mu\text{-H})$ (**3**). The Pd atom occupies the center of the ring. The Pd atom in **5** can be removed reversibly to yield the palladium-free heterocycle $[\text{Re}_2(\text{CO})_8(\mu\text{-SbPh}_2)(\mu\text{-H})]_2$ (**6**).



INTRODUCTION

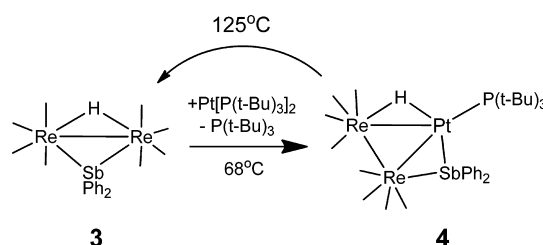
In recent studies, our group¹ and others^{2,3} have synthesized several unusual new metalloheterocycles by linking heavy transition-metal groupings with heavy-atom bridging ligands, such as diphenylantimony and diphenylbismuth, derived from the main group elements. Among these are the five- and six-membered rhenium-heterocycles $\text{HPtRe}_2(\text{CO})_8[\text{P}(t\text{-Bu})_3]_2(\mu\text{-SbPh}_2)_2(\mu\text{-H})$ (see ref 1a) (**1**) and $[\text{Re}(\text{CO})_3(\mu\text{-BiPh}_2)]_3$ (see ref 1b) (**2**).



The 3-membered heterocycle $\text{Re}_2(\text{CO})_8(\mu\text{-SbPh}_2)(\mu\text{-H})$ (see ref 4) (**3**) has been shown to undergo a reversible ring-opening insertion of a $\text{Pt}[\text{P}(t\text{-Bu})_3]$ group into one of its Re–Sb bonds to yield the Re_2Pt complex $\text{Re}_2\text{Pt}[\text{P}(t\text{-Bu})_3](\text{CO})_8(\mu\text{-SbPh}_2)(\mu\text{-H})$ (**4**) upon reaction with $\text{Pt}[\text{P}(t\text{-Bu})_3]_2$ (see Scheme 1).⁵

We have now found that, when solutions of **3** are heated to 45 °C in the presence of $\text{Pd}(\text{dba})_2$ (where dba = dibenzylideneacetone), **3** undergoes a remarkable ring-opening dimerization to form the new six-membered heterocyclic complex $\text{PdRe}_4(\text{CO})_{16}(\mu\text{-SbPh}_2)_2(\mu\text{-H})_2$ (**5**) that contains a single Pd atom in the center of the ring. In a process reminiscent of host–guest behavior, it has been found that the Pd atom in **5**, that is formally uncharged, can be removed by treatment with phosphine ligands to yield the palladium-free heterocycle $\text{Re}_4(\text{CO})_{16}(\mu\text{-SbPh}_2)_2(\mu\text{-H})_2$ (**6**), and then added

Scheme 1



again by treatment with $\text{Pd}(\text{dba})_2$ to regenerate **5**. Host–guest phenomena have been an effective method for gaining control over the reactivity of ions, molecules, metal complexes, and nanomaterials in recent years.^{6–10} Herein, we report on the reactions of **3** with the palladium sources $\text{Pd}(\text{dba})_2$ and $\text{Pd}(\text{P}(t\text{-Bu})_3)_2$ and our studies of the transformations of palladium-free heterocycle $\text{Re}_4(\text{CO})_{16}(\mu\text{-SbPh}_2)_2(\mu\text{-H})_2$ (**6**). A preliminary report of this work has been published.¹¹

EXPERIMENTAL DETAILS

General Data. Reagent-grade solvents were dried by the standard procedures and were freshly distilled prior to use. Infrared spectra were recorded on a Thermo Nicolet Avatar 360 FT-IR spectrophotometer. ¹H NMR spectra were recorded on a Varian Mercury 300 spectrometer operating at 300.1 MHz. Mass spectrometric (MS) measurements performed by a direct-inlet probe by using electron impact ionization (EI) were made on a VG 70S instrument. $\text{Pd}(\text{P}(t\text{-Bu})_3)_2$, $\text{Pd}(\text{dba})_2$, dba = $\text{O}=\text{C}(\text{CH}=\text{CHC}_6\text{H}_5)_2$, SbPh_3 and $\text{Re}_2(\text{CO})_{10}$ were purchased from STREM and were used without

Received: January 15, 2015

Published: March 10, 2015



further purification. $\text{Re}_2(\text{CO})_8(\mu\text{-SbPh}_2)(\mu\text{-H})$, **3** was prepared according to a previously reported procedure.⁴ Product separations were performed by TLC in air on Analtech 0.25 and 0.5 mm silica gel 60 Å F_{254} on glass plates.

Reaction of $\text{Re}_2(\text{CO})_8(\mu\text{-H})(\mu\text{-SbPh}_2)$ with $\text{Pd}(\text{dba})_2$. 30.0 mg (0.0343 mmol) of $\text{Re}_2(\text{CO})_8(\mu\text{-H})(\mu\text{-SbPh}_2)$ was added to 11.8 mg (0.0206 mmol) of $\text{Pd}(\text{dba})_2$ in 0.4 mL of benzene and sealed under vacuum in a test tube. The reaction solution was heated to 50 °C for 3 h. Upon cooling orange-red crystals consisting of a co-crystallized mixture of $\text{PdRe}_4(\text{CO})_{16}(\mu\text{-SbPh}_2)_2(\mu\text{-H})_2$ (**5**) and $\text{Re}_4(\text{CO})_{16}(\mu\text{-SbPh}_2)_2(\mu\text{-H})_2$ (**6**) formed. The reaction solution was decanted and the crystals were washed three times with benzene. These crystals of **5** always contain some **6**. The mixture of **5** and **6** was 11.1 mg (33% yield). 1.2 mg of $\text{Pd}_2\text{Re}_4(\text{CO})_{16}(\mu\text{-Ph})(\mu_4\text{-SbPh})(\mu_3\text{-SbPh}_2)(\mu\text{-H})_2$, **7** (6% yield) was also obtained from the remaining reaction solution by workup by TLC by using a 3:1 hexane/methylene chloride solvent mixture for elution. Colorless **6** can be separated from orange **5** in a pure form with considerable loss of material by dissolving the mixed crystals of **5** and **6** in CH_2Cl_2 and separating by TLC in air by using a 3:1 hexane/methylene chloride solvent mixture for elution. With pure **6** in hand, the spectral features of **5** in the samples that contain both **5** and **6** could be unambiguously assigned. Spectral data for **5**: IR ν_{CO} (cm^{-1} in methylene chloride): 2082(s), 2016(vs), 1994(m), 1981(s), 1952(m). ^1H NMR ($\text{CD}_3\text{C}_6\text{D}_5$, in ppm) δ = 7.10 (m, 20H, Ph), −17.89 (s, 2H, hydride). Spectral data for **6**: IR ν_{CO} (cm^{-1} in methylene chloride): 2093(s), 2021(vs), 1999(m), 1983(s), 1956(m). ^1H NMR (CD_2Cl_2 , in ppm) δ = 7.39–7.61 (m, 20H, Ph), −14.94 (s, 2H, hydride). Mass spectroscopy (EI/MS) m/z 1746. The isotope distribution pattern is consistent with the presence of four Re atoms and two Sb atoms. The ratio of **6/5** in samples containing enough material for a ^1H NMR spectroscopic analysis is easily determined by the intensity ratio of their hydride resonances, δ = −14.94 for **6** and −17.89 for **5**. Spectral data for **7**. IR ν_{CO} (cm^{-1} in hexane): 2098(m), 2076(s), 2015(vs), 2008(s), 2002(s), 1996(s), 1984(s), 1966(m), 1959(m), 1936(w). ^1H NMR (CD_2Cl_2 , in ppm) δ = 7.05–7.71 (m, 20H, Ph), −11.97 (d, 1H, J = 4.3 Hz, Re–H–Pd), −15.11 (d, 1H, J = 4.3 Hz, Pd–H–Pd). Mass spectroscopy (EI/MS) m/z 1960. The isotope distribution pattern is consistent with the presence of four Re atoms, two Sb atoms, and two Pd atoms.

Reaction of **3 with $\text{Pd}(\text{P}(t\text{-Bu})_3)_2$.** 40.0 mg (0.0457 mmol) of **3** was added to 5.8 mg (0.0114 mmol) of $\text{Pd}(\text{P}(t\text{-Bu})_3)_2$ and dissolved in 0.2 mL of benzene and sealed under vacuum in a test tube. The reaction was heated for 3 h at 50 °C. Yellow crystals formed. The solvent was decanted, washed with 2 mL of benzene followed by a 2 mL of 1:1 benzene/hexane solvent mixture. 11.9 mg (29% yield) of pure colorless **6** was obtained by crystallization in air. The mother liquor and washes were combined and then worked up by thin-layer chromatography (TLC), using a 3:1 hexane/methylene chloride solvent mixture to yield 1.7 mg (4% yield) of red **7**.

Heating $\text{Re}_2(\text{CO})_8(\mu\text{-H})(\mu\text{-SbPh}_2)$ in the Absence of Pd. 10.0 mg (0.0114 mmol) of **3** was dissolved in 1.0 mL of $\text{C}_6\text{D}_5\text{CD}_3$ in a 5-mm NMR tube. The NMR tube was evacuated and filled with nitrogen five times. It was then heated to 110 °C for 4 h. After this period, there was no NMR spectroscopic evidence for the formation of any **6**.

Removal of Pd from **5 To Yield **6**.** 2.0 mg (0.0011 mmol) of **5** and 1.5 mg (0.0053 mmol) of $\text{P}(c\text{-C}_6\text{H}_{11})_3$ were dissolved in CD_2Cl_2 . At t = 0 h, the solution contained 88% of **5** and 12% of **6**. At t = 3 h, the solution contained 5% **5** and 95% **6**.

Addition of Pd to **6 To Yield **5**.** 2.0 mg (0.0011 mmol) of **6**, 3.3 mg (0.0057 mmol) of $\text{Pd}(\text{dba})_2$, and 3.8 mg (0.0051 mmol) of $\text{H}_4\text{Ru}_4(\text{CO})_{12}$ (added for use as an internal standard) were dissolved in CD_2Cl_2 and placed in a NMR tube. The NMR tube then was cooled to −21 °C and maintained at this temperature. At the start, the solution contained 96% **6** and 4% **5**. After 24 h, the solution contained 57% **6** and 43% **5**.

Pyrolysis of **6 at 85 °C.** Under nitrogen, a 35.0 mg portion of **6** was dissolved in 5 mL of freshly distilled toluene in a small three-neck flask and was heated to 85 °C in a constant-temperature oil bath for 24 h. After cooling, the solvent was removed *in vacuo*, and the residue was then extracted in methylene chloride and separated by TLC by using a

4:1 hexane/methylene chloride (v/v) solvent mixture. The isolated products listed in order of elution include: a colorless band of **3**, 1.4 mg (4% yield), a colorless band of $\text{Re}_3(\text{CO})_{12}(\mu\text{-SbPh}_2)(\mu\text{-H})_2$ (**8**), 0.9 mg (3% yield), a colorless band of $\text{Re}_2(\text{CO})_8(\mu\text{-SbPh}_2)_2$,¹² 0.8 mg (2% yield), a colorless band of $\text{Re}_3(\text{CO})_{12}(\mu\text{-SbPh}_2)_2(\mu\text{-H})$ (see ref 13) (**9**), 9.7 mg (25% yield), a yellow band of $\text{Re}_3(\text{CO})_{13}(\mu\text{-SbPh})(\mu\text{-H})$ (see ref 13) (**10**), 4.4 mg (15% yield). Small amounts of $\text{H}_3\text{Re}_3(\text{CO})_{12}$ were detected spectroscopically in reaction solutions that were monitored by ^1H NMR spectroscopy. Spectral data for **8**: IR (ν_{CO} cm^{-1} in hexane): 2114(w), 2084(s), 2022(vs), 2006(m), 1987(m), 1973(m). ^1H NMR (CD_2Cl_2 , in ppm) δ = 7.5–7.3 (m, 10H, Ph), −19.2 (s, 2H, hydride). Mass Spectroscopy (EI/MS): 1172(M^+), 1144($\text{M}^+ - \text{CO}$), 1116($\text{M}^+ - 2\text{CO}$), 1088($\text{M}^+ - 3\text{CO}$) m/z . The isotope distribution pattern is consistent with the presence of three Re atoms and one Sb atom. Spectral data for **9**: IR (ν_{CO} cm^{-1} in hexane): 2101(w), 2076(s), 2013(vs), 1995(s), 1984(m), 1979(m), 1970(m), 1964(w). ^1H NMR (CD_2Cl_2 , in ppm) δ = 7.5–7.2 (m, 10H, Ph), −12.7 (s, 1H, hydride). Mass Spectroscopy (EI/MS): 1448(M^+) m/z . The isotope distribution pattern is consistent with the presence of three Re and two Sb atoms. Spectral data for **10**: IR (ν_{CO} cm^{-1} in hexane): 2132(w), 2093(m), 2073(m), 2038(vs), 2032(s), 2011(m), 2005(s), 1990(vs), 1960(s). ^1H NMR (300 MHz, CDCl_3 , 25 °C, TMS, in ppm) δ = 7.9–7.2 (m, 5H, Ph), −15.8 (s, 1H, hydride). Mass spectroscopy (EI/MS): 1122(M^+), 1066 ($\text{M}^+ - 2\text{CO}$), 1038($\text{M}^+ - 3\text{CO}$), 1010($\text{M}^+ - 4\text{CO}$) m/z . The isotope distribution pattern is consistent with the presence of three Re atoms and one Sb atom.

Crystallographic Analyses. Orange-red single crystals of a **5/6** combination suitable for X-ray diffraction (XRD) analyses were obtained from the reaction solution when it was cooled to room temperature. Colorless single crystals of **6** suitable for XRD analyses were obtained from purified samples by recrystallization from methylene chloride/hexane solvent mixtures by slow evaporation of solvent. Red single crystals of **7** suitable for XRD analyses were obtained by slow evaporation of solvent from hexane at room temperature. Colorless single crystals of **8**, **9**, and **10** suitable for XRD analyses were obtained from solutions of the pure compounds in hexane/methylene chloride solvent mixture by slow evaporation of solvent at −25 °C. Each data crystal was glued onto the end of a thin glass fiber. X-ray intensity data were obtained by using a Bruker SMART APEX CCD-based diffractometer using Mo $K\alpha$ radiation (λ = 0.71073 Å). The raw data frames were integrated with the SAINT+ program by using a narrow-frame integration algorithm.¹⁴ Corrections for Lorentz and polarization effects were also applied with SAINT+. For each analysis, an empirical absorption correction based on the multiple measurement of equivalent reflections was applied by using the program SADABS. All structures were solved by a combination of direct methods and difference Fourier syntheses, and refined by full-matrix least-squares on F^2 by using the SHELXTL software package.¹⁵ All non-hydrogen atoms were refined with anisotropic displacement parameters. Hydrogen atoms on the phenyl groups were placed in geometrically idealized positions and included as standard riding atoms during the final least-squares refinements. The crystals containing mixtures of **5** and **6** crystallized in the orthorhombic crystal system. The space group *Fdd2* was uniquely identified by the pattern of systematic absences observed in the data. The hydride ligands in the **5/6** crystal were located and independently refined in the analysis with an isotropic thermal parameter. This crystal was found to be a co-crystallized mixture of **5** and **6**. In the final stages of refinement, the occupancy factor of the Pd atom was refined and it converged to a value of 0.51. The pure form of compound **6** crystallized in the monoclinic crystal system. The systematic absences in the data were consistent with the space groups *Cc* and *C2/c*. The latter was initially selected and was confirmed by the successful solution and refinement of the structure. The hydride ligands in **6** were refined on their positional parameters with a fixed thermal parameter. Compound **7** crystallized in the triclinic crystal system. The centrosymmetric space group *P1* was selected and was confirmed by the successful solution and refinement of the structure. The hydride ligands in **7** were refined as follows: H1 was refined with the Re–H and Pd–H distances fixed at 1.75 Å. H2 was refined without any restraints. Compound **8**

Table 1. Crystallographic Data for Compounds 5–10^a

	5	6	7
empirical formula	Re ₄ Sb ₂ Pd _{0.5} O ₁₆ C ₄₀ H ₂₂	Re ₄ Sb ₂ O ₁₆ C ₄₀ H ₂₂	Re ₄ Sb ₂ Pd ₂ O ₁₆ C ₄₀ H ₂₂
formula weight	1839.13	1746.88	1959.6
crystal system	orthorhombic	monoclinic	triclinic
lattice parameters			
<i>a</i> (Å)	35.2421(15)	19.9667(18)	10.8973(15)
<i>b</i> (Å)	52.7954(19)	13.5280(12)	11.0822(15)
<i>c</i> (Å)	10.2274(4)	19.2161(17)	22.043(3)
α (deg)	90.00	90.00	94.339(2)
β (deg)	90.00	118.476(2)	91.570(3)
γ (deg)	90.00	90.00	114.493(2)
<i>V</i> (Å ³)	19029.3(13)	4562.5(7)	2410.5(6)
space group	<i>Fdd2</i>	<i>C2/c</i>	<i>P</i> $\bar{1}$
<i>Z</i>	16	4	2
ρ_{calc} (g/cm ³)	2.568	2.543	2.700
μ (Mo <i>K</i> α) (mm ^{−1})	11.506	11.804	11.894
temperature (K)	100(2)	294(2)	294(2)
$2\theta_{\text{max}}$ (deg)	50.06	56.12	50.70
No. obs (<i>I</i> > 2 σ (<i>I</i>))	7447	4030	4771
No. of parameters	566	284	584
goodness of fit, GOF	1.037	1.044	0.965
max. shift in cycle	0.001	0.001	0.001
residuals*: <i>R</i> ₁ ; <i>wR</i> ₂	0.0356; 0.0692	0.0247; 0.0465	0.0667; 0.1372
absorption correction, max/min	multiscan 1.000/0.853	multiscan 1.000/0.741	multiscan 1.000/0.097
largest peak in final diff. map (e [−] /Å ³)	1.028	0.898	2.874
^a <i>R</i>			
	8	9	10
empirical formula	Re ₃ SbO ₁₂ C ₂₄ H ₁₂	Re ₃ Sb ₂ O ₁₂ C ₃₆ H ₂₁	Re ₃ SbO ₁₃ C ₁₉ H ₆
formula weight	1172.69	1447.63	1122.59
crystal system	triclinic	triclinic	monoclinic
lattice parameters			
<i>a</i> (Å)	13.6204(8)	16.0769(7)	10.3134(5)
<i>b</i> (Å)	19.0089(12)	17.2298(7)	14.3792(7)
<i>c</i> (Å)	20.2437(13)	18.7642(8)	18.3407(9)
α (deg)	99.870(1)	100.110(1)	90
β (deg)	106.934(1)	107.714(1)	90.571(1)
γ (deg)	109.933(1)	117.632(1)	90
<i>V</i> (Å ³)	4495.0(5)	4066.1(3)	2719.8(2)
space group	<i>P</i> $\bar{1}$	<i>P</i> $\bar{1}$	<i>P</i> ₂ /m
<i>Z</i>	6	4	4
ρ_{calc} (g/cm ³)	2.599	2.635	2.742
μ (Mo <i>K</i> α) (mm ^{−1})	13.027	10.266	14.349
temperature (K)	294(2)	294(2)	294(2)
$2\theta_{\text{max}}$ (deg)	52.74	52.04	56.60
No. Obs (<i>I</i> > 2 σ (<i>I</i>))	12944	10944	7010
No. of parameters	1105	963	355
goodness of fit, GOF	1.047	1.015	1.213
max. shift in cycle	0.001	0.002	0.001
residuals*: <i>R</i> ₁ ; <i>wR</i> ₂	0.0407; 0.0952	0.0483; 0.0795	0.0400; 0.0933
absorption correction, max/min	multiscan 1.000/0.468	multiscan 1.000/0.657	multiscan 1.000/0.223
largest peak in final diff. map (e [−] /Å ³)	2.321	1.864	1.489

$$^a R = \sum_{hkl} (|F_{\text{obs}}| - |F_{\text{calc}}|) / \sum_{hkl} |F_{\text{obs}}|; R_w = [\sum_{hkl} w(|F_{\text{obs}}| - |F_{\text{calc}}|)^2 / \sum_{hkl} w F_{\text{obs}}^2]^{1/2}; w = 1/\sigma^2(F_{\text{obs}}); \text{GOF} = [\sum_{hkl} w(|F_{\text{obs}}| - |F_{\text{calc}}|)^2 / (n_{\text{data}} - n_{\text{vari}})]^{1/2}.$$

crystallized in the triclinic space group. The hydrides were refined as follows: H1 was refined with the Re1–H1 and Re2–H1 bond distances fixed at 1.75 Å. Compound **9** also crystallized in the triclinic system. The hydride ligand was located along the Re–Re bond and refined on its positional parameter with a fixed isotropic thermal parameter. Compound **10** crystallized in the monoclinic crystal system. The systematic absences in the intensity data for **10** were consistent with the space groups *P*₂₁ and *P*₂₁/m. *P*₂₁/m was selected and confirmed by the successful solution and refinement of the

structure. Crystal data, data collection parameters, and results of the analyses are listed in Table 1.

Computational Analyses. Density functional theory (DFT) calculations were performed with the Amsterdam Density Functional (ADF) suite of programs,¹⁶ using the PBEsol functional with Zero Order Relativistic Approximation (ZORA). Valence quadruple- ζ + 4 polarization, relativistically optimized (QZ4P) basis sets were used for Pd, Re, Sb, O, C, and H atoms with no frozen cores. The molecular orbitals for **5** and **6** and their energies were obtained by geometry-

optimized calculations that were initiated on their respective structures based on their structures obtained from single-crystal XRD analyses. The fragment analysis for compound **5** was also performed with the ADF programs by using the meta-Generalized Gradient Approximation (meta-GGA) level nonempirical Tao–Perdew–Staroverov–Scuseria (TPSS) functional.¹⁷ The above-mentioned basis sets were used.

RESULTS AND DISCUSSION

The reaction of **3** with $\text{Pd}(\text{dba})_2$ in benzene for 3 h at 50 °C yielded orange-red crystals consisting of a mixture yielded the two products **5** and **6** in a combined yield of 33% which co-crystallized from the reaction solution in the same crystal. Compound **6** can be isolated in a pure form by TLC on silica gel albeit with considerable loss. Small amounts of the dipalladium compound **7** were also isolated in low yields (6%) by TLC after work up of the material in the remaining reaction solutions. Compound **6** was also obtained and isolated in 29% yield from the reaction of **3** with $\text{Pd}[\text{P}(t\text{-Bu})_3]_2$ in benzene solvent. In this reaction, no **5** was obtained but a 4% yield of **7** was obtained.

A crystal containing a mixture of **5** and **6** was analyzed by a single-crystal XRD analysis. Compounds **5** and **6** occupy the same sites in this structure. An ORTEP diagram of the superimposed **5/6** combination is shown in Figure 1. The

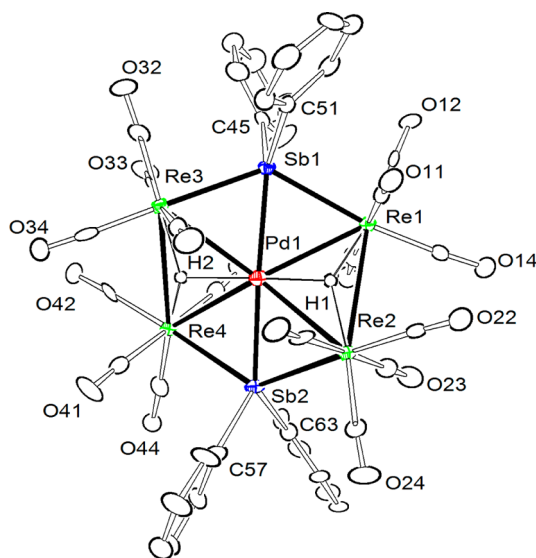


Figure 1. An ORTEP diagram of the molecular structure of **5/6**, showing 30% thermal ellipsoid probabilities. Selected interatomic distances (Å) are as follow: $\text{Re}(1)\text{--Re}(2) = 3.4235(7)$, $\text{Re}(3)\text{--Re}(4) = 3.3592(6)$, $\text{Pd}(1)\text{--Re}(1) = 2.9348(18)$, $\text{Pd}(1)\text{--Re}(2) = 2.9455(19)$, $\text{Pd}(1)\text{--Re}(3) = 2.9820(18)$, $\text{Pd}(1)\text{--Re}(4) = 2.9823(19)$, $\text{Re}(1)\text{--Sb}(1) = 2.7825(10)$, $\text{Re}(2)\text{--Sb}(2) = 2.8007(10)$, $\text{Pd}(1)\text{--Sb}(1) = 2.6306(18)$, $\text{Pd}(1)\text{--Sb}(2) = 2.6351(18)$, $\text{Pd}(1)\text{--H}(1) = 1.90(10)$, $\text{Pd}(1)\text{--H}(2) = 1.76(10)$, $\text{Re}(1)\text{--H}(1) = 1.92(10)$, $\text{Re}(2)\text{--H}(1) = 1.67(10)$, $\text{Re}(3)\text{--H}(2) = 2.05(9)$, $\text{Re}(4)\text{--H}(2) = 1.75(10)$.¹¹

palladium atom appears in the form of a partial occupancy in the center of a six-membered heterocyclic Re_4Sb_2 ring. This particular crystal contained 51% Pd in the center of the Re_4Sb_2 ring, as determined by occupancy refinement. Each Re atom contains four linear terminal carbonyl ligands. Each Sb atom contains two phenyl groups. The SbPh_2 groups lie on opposite sides of the ring

The Pd atom is bonded to all four Re atoms, $\text{Pd}(1)\text{--Re}(1) = 2.9348(18)$ Å, $\text{Pd}(1)\text{--Re}(2) = 2.9455(19)$ Å, $\text{Pd}(1)\text{--Re}(3) = 2.9820(18)$ Å, $\text{Pd}(1)\text{--Re}(4) = 2.9823(19)$ Å, the two Sb atoms, and the two bridging hydrido ligands.¹⁸ The Re–Re bond distances, $\text{Re}(1)\text{--Re}(2) = 3.4235(7)$ Å, $\text{Re}(3)\text{--Re}(4) = 3.3592(6)$ Å, are longer than the Re–Re bond in **3**, $\text{Re}(1)\text{--Re}(2) = 3.2244(6)$ Å⁴ and considerably longer than the Re–Re single-bond distance observed in $\text{Re}_2(\text{CO})_{10}$ (3.041(1) Å).¹⁹ The Re–Sb distances, $\text{Re}(1)\text{--Sb}(1) = 2.7439(17)$ Å, $\text{Re}(2)\text{--Sb}(1) = 2.7434(18)$ Å, $\text{Re}(3)\text{--Sb}(2) = 2.8004(10)$ Å, $\text{Re}(4)\text{--Sb}(1) = 2.8115(10)$ Å are significantly longer than those in **3**, 2.6934(7)–2.6983(7) Å.⁴ The Pd–Sb distances, $\text{Pd}(1)\text{--Sb}(1) = 2.6306(18)$ Å, $\text{Pd}(1)\text{--Sb}(2) = 2.6351(18)$ Å, are short enough to imply significant bonding interactions between these atoms. The Pd–Sb bond distances in the compounds $\text{Pd}(\text{SbPh}_3)_2(\text{Ph})\text{X}$, X = Cl and Br, are 2.5568(5) Å and 2.5421(5) Å, respectively.²⁰ The two equivalent hydride ligands, $\delta = -17.89$, were located and refined in this low-temperature structural analysis, and they serve as triply bridging ligands across the two oppositely positioned Re_2Pd triangles, $\text{Pd}(1)\text{--H}(1) = 1.90(10)$ Å, $\text{Pd}(1)\text{--H}(2) = 1.76(10)$ Å. The nature of the bonding of the Pd atom to the heterocycle was investigated by geometry-optimized DFT molecular orbital calculations and is described below.

Compound **6** can be obtained in a pure crystalline form by TLC of the **5/6** mixtures. Interestingly, compound **6** crystallizes in a different space group than the **5/6** mixed crystals. An ORTEP diagram of the molecular structure of **6** in the solid state is shown in Figure 2.

The structure of compound **6** consists of a puckered six-membered $\text{Re}_2\text{SbRe}_2\text{Sb}$ ring similar to that of **5**. The molecule contains 2-fold rotational symmetry in the solid state. The hydride-bridged Re–Re bond distances, $\text{Re}(1)\text{--Re}(2) =$

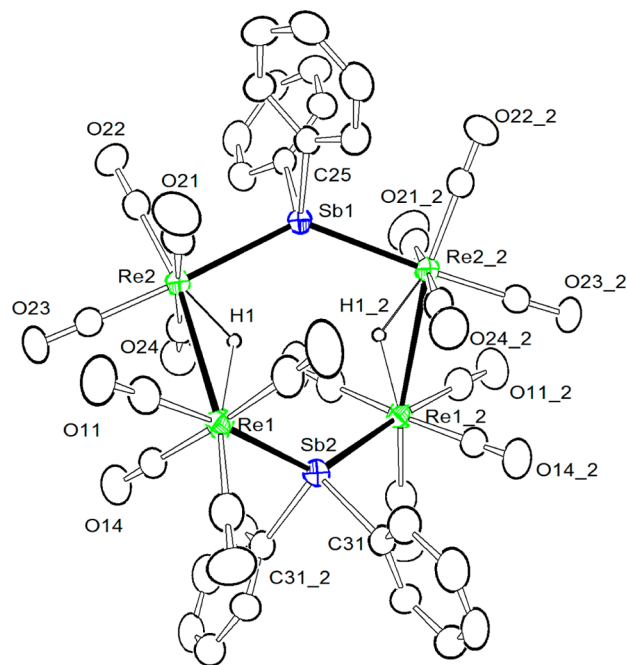


Figure 2. ORTEP diagram of the molecular structure of compound **6** showing 30% thermal ellipsoid probabilities. Selected interatomic bond distances (Å) are as follow: $\text{Re}1\text{--Re}2 = 3.2607(4)$, $\text{Re}1\text{--Sb}2 = 2.8002(4)$, $\text{Re}2\text{--Sb}1 = 2.7959(3)$, $\text{Re}1\text{--H}1 = 2.02(5)$, $\text{Re}2\text{--H}1 = 1.65(5)$.¹¹

3.2607(4) Å, and the Re–Sb bond distances, Re1–Sb2 = 2.8002(4) Å, Re2–Sb1 = 2.7959(3) Å, are significantly shorter than the corresponding distances in **5**. Like **5**, the heterocycle of pure **6** exhibits a chairlike conformation, but in pure **6** it is more puckered than that in **5/6** mixed crystal. The two hydrido ligands are equivalent, $\delta = -14.94$ in the ^1H NMR spectrum, and they bridge the Re–Re bonds on the interior of the ring. Significantly, we could not obtain any evidence for the formation of **6** from **3** in the absence of a source of palladium, even by heating to 100 °C for 2 h.

Compound **7** was also characterized crystallographically. An ORTEP diagram of the molecular structure of **7** is shown in Figure 3. Compound **7** contains two mutually bonded Pd

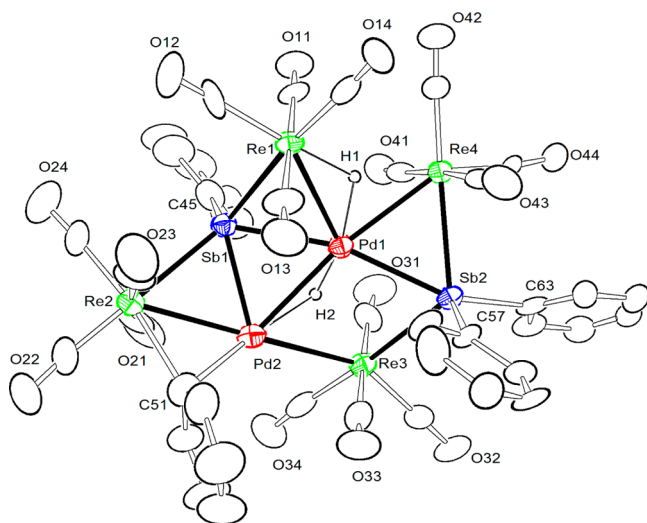


Figure 3. An ORTEP diagram of the molecular structure of **7**, showing 30% thermal ellipsoid probabilities. Selected interatomic bond distances (Å) are as follow: Re(1)–Sb(1) = 2.7439(17), Re(1)–Pd(1) = 2.9317(18), Re(2)–Sb(1) = 2.7434(18), Pd(1)–Pd(2) = 2.848(2), Re(2)–Pd(2) = 2.839(2), Re(3)–Pd(2) = 2.961(2), Re(3)–Pd(1) = 3.0949(19), Re(4)–Pd(1) = 2.7895(19), Re(4)–Sb(2) = 2.8527(17), Pd(1)–Sb(2) = 2.736(2), Pd(2)–Sb(1) = 2.574(2), Pd(1)–Sb(1) = 2.666(2), Re(2)–C(51) = 2.31(3), Pd(2)–C(51) = 2.16(3), Pd(1)–H(1) = 1.75(1), Re(1)–H(1) = 1.75(1), Re(3)–H(2) = 2.11(14), Pd(1)–H(2) = 1.37(14), Pd(2)–H(2) = 1.83(14).¹¹

atoms. Formally, **7** contains two ring-opened equivalents of **3**, but they are separated by the two added Pd atoms and one of the phenyl rings was cleaved from one of the original SbPh₂ ligands to become a bridging ligand across the Re(2)–Pd(2) bond. The SbPh remnant serves as quadruply bridging ligand by bonding to two of the Re atoms and both of the Pd atoms. The Pd atoms are mutually bonded, Pd(1)–Pd(2) = 2.848(2) Å. The cleaved phenyl ring has adopted a semibridging position across the Re(2)–Pd(2) bond, Re(2)–C(51) = 2.31(3) Å, Pd(2)–C(51) = 2.16(3) Å. Many complexes containing semibridging phenyl ligands have appeared recently.²¹ The SbPh₂ ligand in **7** is a triply bridging ligand bonded to Re(3), Pd(1), and Re(4). It resembles the two triply bridging SbPh₂ ligands found in **5** except that the Pd–Sb distance, Pd(1)–Sb(2) = 2.736(2) Å, in **7** is significantly longer than that in **5**.

Compound **7** contains two hydrido ligands: one bridges the Pd(1)–Re(1) bond, Pd(1)–H(1) = 1.75(1) Å, Re(1)–H(1) = 1.75(1) Å; the other one H(2) is a semitriple bridge on the Re(3), Pd(1), Pd(2) triangle, Pd(1)–H(2) = 1.37(14) Å,

Pd(2)–H(2) = 1.83(14) Å. Re(3)–H(2) = 2.11(14) Å. On the basis of its formula, it appears that **7** was formed from **5** by the addition of one Pd atom accompanied by the cleavage of one phenyl group from one of the SbPh₂ ligands, but since we have been unable to obtain **5** in a pure form, we have been unable to confirm this hypothesis.

In order to gain a better understanding of the nature of the bonding of the Pd atom to the ring in compound **5**, geometry-optimized DFT calculations were performed on both **5** and **6**. The molecular orbitals (MOs) of **6** will be described first, and these are shown in Figure 4. The HOMO of **6** shows bonding

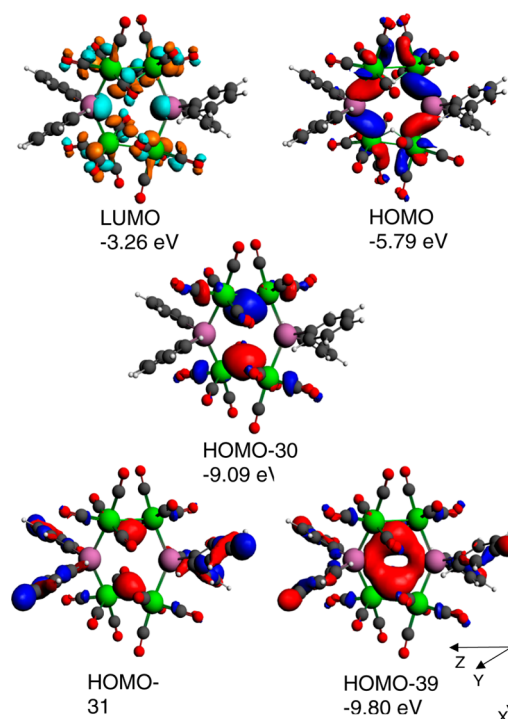


Figure 4. Selected molecular orbitals for **6** and their respective calculated energies (in eV).

interactions between what are formally the p_x orbitals on the two Sb atoms and the $d_{x^2-y^2}$ orbitals on the Re atoms. HOMO-30 and HOMO-31 show the bonding of the hydrido ligands to the Re atoms. This bonding is a combination of the 1s orbitals of the H atoms with the d_{xz} orbitals of the Re atoms. This molecular orbital can be viewed as a combination of two three-center two-electron Re–H–Re bonds. HOMO-39 is an interesting molecular orbital that shows the nature of the Re–Sb bonding across the entire six-membered ring. This molecular orbital, shaped like a doughnut, includes the 1s orbital from each H ligand, the p_z orbitals on the two Sb atoms and the d_{xz} orbitals from the four Re atoms. This highly delocalized orbital lies a low energy (−9.80 eV) and greatly stabilizes the structure of the ring.

The molecular orbitals of **5** are shown in Figure 5. The interaction between the Pd atom and the heterocycle **6** is nicely illustrated by HOMO-29, which shows strong interactions between the Pd d_{xy} orbital and the HOMO of the ring.

Interactions between the Pd atom and the two hydrido ligands are shown in HOMO-40 and HOMO-52, which are formed principally by interactions of the d_{xz} and p_x orbitals on Pd with the HOMO-30 of **6** and the d_{z^2} and s orbitals on Pd and HOMO-31 of **6**, respectively. The HOMO-30 and

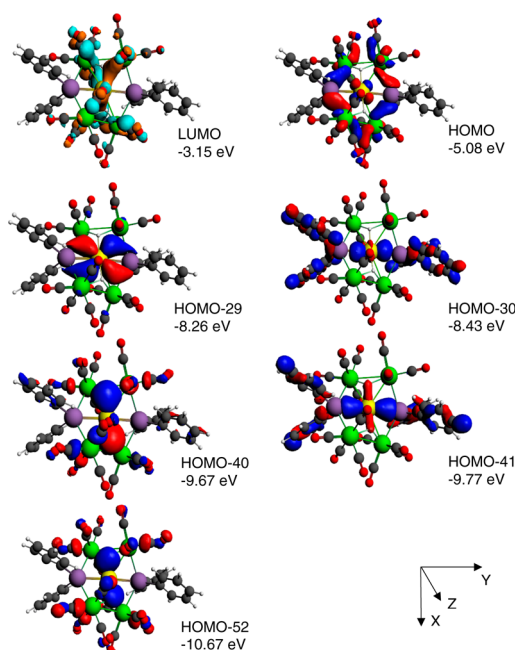


Figure 5. Selected molecular orbitals for **5** with the corresponding calculated energies that show important bonding between the central Pd atom and the Re atoms, Sb atoms, and the hydrido ligands of the heterocyclic ring.

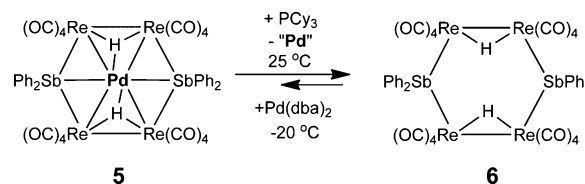
HOMO-41 of **5** also show important interactions between the $d_{x^2-y^2}$ orbital on Pd and the LUMO of **6**. The net bonding interactions, donation from the electron-rich hydrides into the Pd 5s and 5p and donation from the Pd 4d orbitals into the LUMO of **6**, stabilize the molecule to a surprisingly large degree as the neutral Pd atom's binding energy is 40 kcal/mol. A DFT fragment analysis that shows additional Pd/ring interactions in **5** were performed and are provided in the accompanying Supporting Information.

When a solution of a **6/5** mixture (12/88) was treated with PCy_3 , Cy = C_6H_{11} (cyclohexyl), the Pd atom was removed from **5** with conversion to **6** in 3 h at 25 °C; no **5** remained as determined by ^1H NMR spectroscopy. Insertion of the Pd atom back into the ring of **6** was not as facile and most certainly depends on the source of the zerovalent Pd atom and the binding ability of its ligands. As one example, a solution of **5/6** (4/96) in CD_2Cl_2 solvent in an NMR tube was treated with $\text{Pd}(\text{dba})_2$ at -20 °C. After a period of 24 h, the **5/6** ratio increased to 43/57, as determined by the increase in the hydride resonance of **5** at $\delta = -17.89$, relative to that of **6** at $\delta = -14.94$.

The mechanism of the palladium-catalyzed dimerization of **3** to **6** has not yet been fully established, but it seems most likely that it involves a series of insertions of a Pd-containing grouping into one of the Re–Sb bonds in **3**, as was observed in the reaction of **3** with $\text{Pt}[\text{P}(t\text{-Bu})_3]_2$.⁹ This proceeds through a Re–Sb ring-opening addition of a second equivalent of **3** and ring closing cyclization to yield the Pd-stabilized product **5**. More interesting, however, is the observation that the Pd atom can be reversibly removed from **5** (see Scheme 2).

We were unable to obtain **6** by heating **3** in the absence of a source of zerovalent Pd. Thus, the Pd appears to be essential for the formation of the six-membered ring in **5**. Since we were able to isolate **6** in the pure form, we were able to investigate its thermal stability. When a solution of **6** in toluene solvent was

Scheme 2



heated to 85 °C for 24 h, the compounds **3** (4% yield), $\text{Re}_2(\text{CO})_8(\mu\text{-SbPh}_2)_2$ ¹² (2% yield), and three new compounds: $\text{Re}_3(\text{CO})_{12}(\mu\text{-SbPh}_2)(\mu\text{-H})_2$ (**8**) (3% yield), $\text{Re}_3(\text{CO})_{12}(\mu\text{-SbPh}_2)_2(\mu\text{-H})$ (**9**) (25% yield), and $\text{Re}_3(\text{CO})_{13}(\mu\text{-SbPh})(\mu\text{-H})$ (**10**) (15% yield) were formed. Compounds **8**–**10** were each characterized by single-crystal X-ray diffraction analyses, and ORTEP diagrams of their molecular structures are shown in Figures 6–8. There are three independent molecules in the

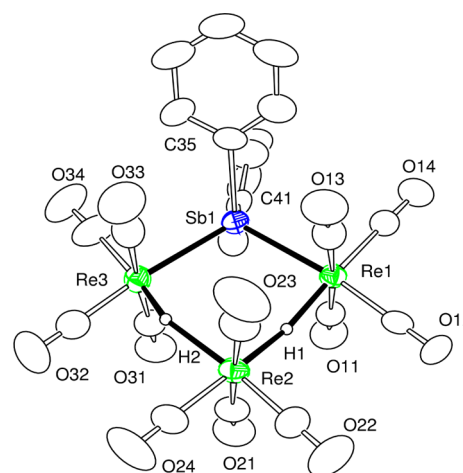


Figure 6. An ORTEP diagram of the molecular structure of $\text{Re}_3(\text{CO})_{12}(\mu\text{-SbPh}_2)(\mu\text{-H})_2$ (**8**), showing 30% thermal ellipsoid probabilities. Selected interatomic bond distances (Å) for the three independent molecules in the crystal are as follow: $\text{Re1–Re2} = 3.4545(6)$, $\text{Re2–Re3} = 3.4387(6)$, $\text{Re1–Sb1} = 2.7525(8)$, $\text{Re3–Sb1} = 2.7527(8)$, $\text{Re1–H1} = 1.74(9)$, $\text{Re2–H1} = 1.75(9)$, $\text{Re2–H2} = 2.05(12)$, $\text{Re3–H2} = 1.49(12)$; $\text{Re4–Re5} = 3.4657(7)$, $\text{Re5–Re6} = 3.4955(7)$, $\text{Re4–Sb3} = 2.7508(8)$, $\text{Re6–Sb3} = 2.7539(9)$, $\text{Re4–H3} = 1.76(2)$, $\text{Re5–H3} = 1.76(2)$, $\text{Re5–H4} = 1.767(18)$, $\text{Re6–H4} = 1.763(18)$; $\text{Re7–Re8} = 3.4314(7)$, $\text{Re8–Re9} = 3.4973(6)$, $\text{Re7–Sb2} = 2.7408(8)$, $\text{Re9–Sb2} = 2.7600(8)$, $\text{Re7–H5} = 1.45(12)$, $\text{Re8–H5} = 2.11(12)$, $\text{Re8–H5} = 2.11(12)$, $\text{Re8–H6} = 1.766(18)$, $\text{Re9–H6} = 1.763(18)$.

crystal of **8**. All of the molecules are structurally similar and consist of a four-membered Re_3Sb ring containing three $\text{Re}(\text{CO})_4$ groups with one bridging SbPh_2 group. The hydride ligands bridge the Re–Re bonds and the Re–Re bonds are long, ranging from 3.4314(7) Å to 3.4973(6) Å. The long length is certainly due in part to the presence of the bridging hydride ligands.²² Compound **8** is structurally similar to its known Bi homologue $\text{Re}_3(\text{CO})_{12}(\mu\text{-BiPh}_2)(\mu\text{-H})_2$, which also has very long hydride-bridged Re–Re bonds, 3.4299(3) Å and 3.5055(3) Å.²³ The Re–Sb distances in **8** (2.7408(8)–2.7600(8) Å) are similar to those found in **3** and are significantly shorter than those found in **5** and **6**. This may be a ring size effect, i.e., the smaller rings have shorter Re–Sb bonds.

Compound **9** contains two independent molecules in the crystal. Both are structurally similar and consist of a five-

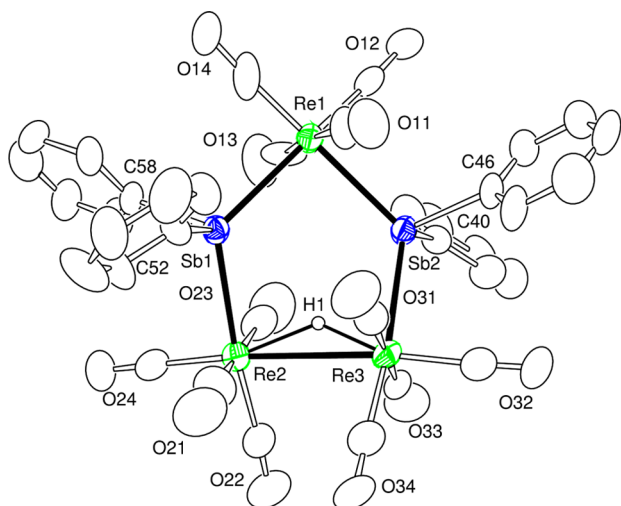


Figure 7. An ORTEP diagram of the molecular structure of $\text{Re}_3(\text{CO})_{12}(\mu\text{-SbPh}_2)_2(\mu\text{-H})$ (**9**), showing 30% thermal ellipsoid probabilities. Selected interatomic bond distances (Å) for the two independent molecules in the crystal are as follow: $\text{Re2-Re3} = 3.2665(7)$, $\text{Re5-Re6} = 3.3000(7)$, $\text{Re1-Sb1} = 2.7820(8)$, $\text{Re1-Sb2} = 2.7718(8)$, $\text{Re2-Sb1} = 2.7780(8)$, $\text{Re3-Sb2} = 2.7639(8)$, $\text{Re4-Sb3} = 2.7885(8)$, $\text{Re4-Sb4} = 2.7745(8)$, $\text{Re5-Sb3} = 2.7972(9)$, $\text{Re6-Sb4} = 2.7727(8)$, $\text{Re2-H1} = 1.747(10)$, $\text{Re3-H1} = 1.748(10)$, $\text{Re5-H2} = 1.745(10)$, $\text{Re6-H2} = 1.747(10)$.

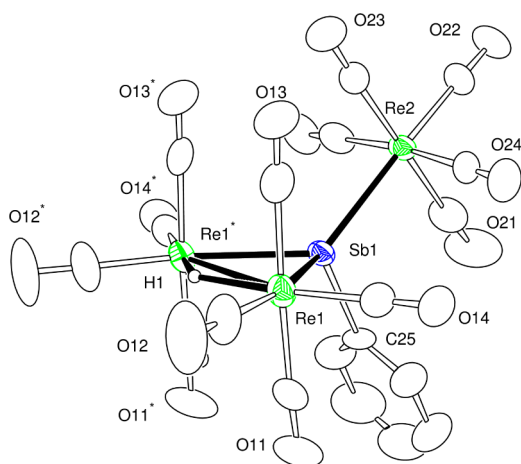


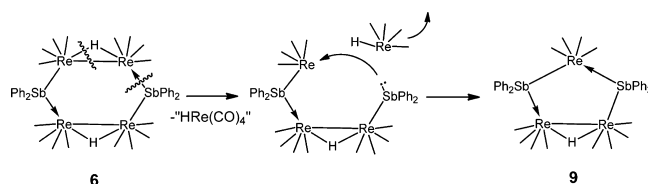
Figure 8. An ORTEP diagram of the molecular structure of $\text{Re}_3(\text{CO})_{13}(\mu_3\text{-SbPh})(\mu\text{-H})$ (**10**), showing 30% thermal ellipsoid probabilities. Selected interatomic bond distances (Å) are as follow: Molecule 1, $\text{Re1-Re1}^* = 3.2284(7)$, $\text{Re1-Sb1} = 2.7337(6)$, $\text{Re2-Sb1} = 2.7854(8)$, $\text{Re1-H1} = 1.81(4)$; Molecule 2, $\text{Re3-Re3}^* = 3.2050(7)$, $\text{Re3-Sb2} = 2.7208(7)$, $\text{Re4-Sb2} = 2.7768(10)$, $\text{Re3-H2} = 1.82(5)$.

membered Re_3Sb_2 ring composed of three $\text{Re}(\text{CO})_4$ groups linked by two bridging SbPh_2 groups. There is one hydride-bridged Re–Re bond in each molecule, $\text{Re-Re} = \text{Re2-Re3} = 3.2665(7)$ Å; $\text{Re5-Re6} = 3.3000(7)$ Å, which is shorter than those in **8**. Interestingly, the hydride ligand lies on the inside of the ring. The Re–Sb bonds are all slightly longer— $2.7820(8)$ Å, $2.7718(8)$ Å, $2.7780(8)$ Å, $2.7639(8)$ Å, $2.7885(8)$ Å, $2.7972(9)$ Å, $2.7727(8)$ Å—than those in the 3- and 4-membered ring compounds **3** and **8**. Compound **9** is structurally similar to the triosmium five-membered compounds $\text{Os}_3(\text{CO})_{12}(\mu\text{-SbR}_2)_2\text{Cl}_2$, $\text{R} = \text{Ph}$, *p*-tolyl that contain two terminally coordinated chloride ligands.^{2a}

The crystal of compound **10** contains two independent molecules. Both molecules are structurally similar and both contain crystallographically imposed reflection symmetry. Compound **10** is structurally similar to the three-membered ring compound **3**, but has a $\text{Re}(\text{CO})_5$ group in the place of one of the phenyl rings on the Sb atom. The SbPh group can be viewed as a bridge across an open cluster of three rhenium carbonyl groups. There are two $\text{Re}(\text{CO})_4$ groups that are mutually bonded, $\text{Re-Re} = 3.2284(7)$ Å [$3.2050(7)$ Å] and contain a bridging hydride ligand. The Re–Sb bond distances to these Re atoms are similar to those in **3**, $2.7337(6)$ Å [$2.7208(7)$ Å]. The Re–Sb bond to the $\text{Re}(\text{CO})_5$ group is significantly longer, $2.7854(8)$ Å [$2.7768(10)$ Å].

Compound **9** is the principal product obtained from the degradation of **6**. Compound **9** could be formed by the elimination of a “ $\text{HRe}(\text{CO})_4$ ” group from **6** (see Scheme 3); in

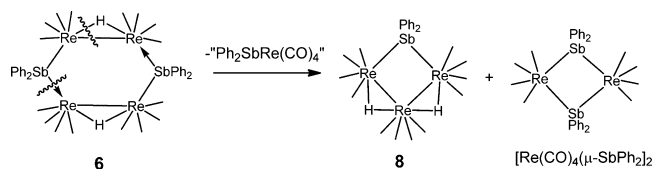
Scheme 3. Loss of a $\text{HRe}(\text{CO})_4$ Group from **6** To Form **9**



all of the following schemes, the CO ligands on the Re atoms are represented simply as lines. Consistent with this, was the observation of the formation of small amounts of $\text{H}_3\text{Re}_3(\text{CO})_{12}$ in the reaction solutions when the thermal degradation of **6** was monitored by ^1H NMR spectroscopy.

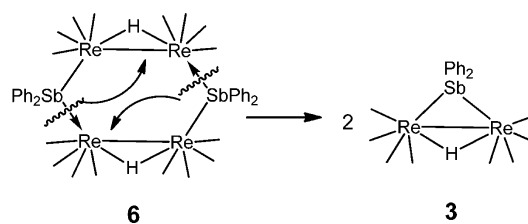
Compound **8** could be formed by the expulsion of a “ $\text{Re}(\text{CO})_4(\text{SbPh}_2)$ ” group from **6**. This is consistent with the formation of small amounts (2% yield) of $[\text{Re}(\text{CO})_4(\text{SbPh}_2)]_2$, a dimer of “ $\text{Re}(\text{CO})_4(\text{SbPh}_2)$ ”, also observed in the degradation of **6** (see Scheme 4).

Scheme 4. Fragmentation of **6** To Form **8** and $\text{Re}_2(\text{CO})_8(\mu\text{-SbPh}_2)_2$



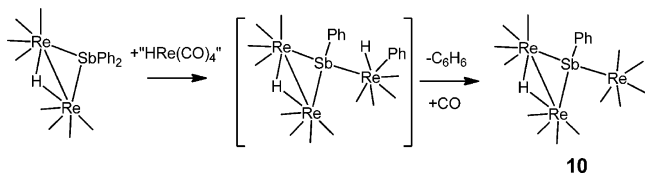
A series of trans-annular Re–Sb bond cleavages in **6** could generate two equivalents of the original compound **3** used for the formation of **5** (Scheme 5). Small amounts of **3** (4% yield) were also observed in the degradation of **6**.

Scheme 5. Two Trans-annular Re–Sb Bond Cleavages in **6** Lead to Two Molecules of **3**



Compound **10** could be formed by the insertion of an $\text{HRe}(\text{CO})_4$ group into an $\text{Re}-\text{Sb}$ bond of **3**, followed by the reductive elimination of benzene and the addition of one equivalent of CO (Scheme 6).

Scheme 6. A Plausible Route to **10**



It has been shown that the unsaturated fragment $\text{Pt}[\text{P}(t\text{-Bu})_3]$ inserts into the SbPh bond of $\text{HRe}(\text{CO})_4(\text{SbPh}_3)$ to yield the SbPh_2 -bridged compound $\text{PtRe}(\text{CO})_4(\text{Ph})[\text{P}(t\text{-Bu})_3](\mu\text{-SbPh}_2)(\mu\text{-H})$.^{1a}

SUMMARY AND CONCLUSIONS

The palladium-containing heterocycle (**5**) was synthesized by a ring-opening cyclization of 2 equiv of compound **3**. Presumably, this proceeds by a series of ring-opening insertions of a Pd atom released from the $\text{Pd}(\text{dba})_2$ precursor into one of the $\text{Re}-\text{Sb}$ bonds of **3**. The palladium clearly stabilizes the heterocyclic Re_4Sb_2 ring through bonds to the Sb and Re atoms and also to the bridging hydrido ligands. Interestingly, the Pd atom can be both removed from the ring when treated with PCy_3 and reinserted into it by treatment with $\text{Pd}(\text{dba})_2$. The Pd -free compound **6** is sufficiently stable for isolation and characterization, but it cannot be formed by thermal treatments of **3** in the absence of palladium. Indeed, when **6** is heated it is degraded by the expulsion of molecular fragments and **3** is one of the degradation products. Compound **3** may indeed be more stable than **6**, although it probably contains some ring strain. Two larger and less-strained ReSb ring systems, **8** and **9**, were also formed in the degradation of **6**.

Perhaps, the most important feature of this study is that compound **6** can be viewed as a host for the complexation of a single, uncharged Pd atom as found in **5**. It is possible that heavy atom metallocycles such as **6**, could serve as a new family of hosts for low-valent including zerovalent metal atom guests that could be delivered to the heterocycles and reversibly retrieved.

ASSOCIATED CONTENT

Supporting Information

Details of the structural analyses of the new compounds, computational analyses, and the final CIF files for each of the structural analyses are available. This material is available free of charge via the Internet at <http://pubs.acs.org>.

AUTHOR INFORMATION

Corresponding Authors

*E-mail: adamsrd@mailbox.sc.edu (R. D. Adams).

*E-mail: hall@chem.tamu.edu (M. B. Hall).

Notes

The authors declare no competing financial interest.

ACKNOWLEDGMENTS

This research was supported by the following grants from the National Science Foundation: Nos. CHE-1111496 and CHE-1048629. The authors from Texas A&M University gratefully

acknowledge the National Science Foundation (Nos. CHE-0910552 and CHE-1300787) and The Welch Foundation (Grant No. A-0648) for support.

REFERENCES

- (1) (a) Adams, R. D.; Pearl, W. C., Jr. *Organometallics* **2010**, *29*, 3887–3895. (b) Adams, R. D.; Pearl, W. C., Jr. *Organometallics* **2009**, *48*, 9519–9525.
- (2) (a) Li, Y.-Z.; Ganguly, R.; Leong, W. K. *Organometallics* **2014**, *33*, 3867–3876. (b) Fenske, D.; Rothenberger, A.; Wieber, S. *Eur. J. Inorg. Chem.* **2007**, 3469–3471.
- (3) Leong, W. K.; Chen, G. J. *Chem. Soc., Dalton Trans.* **2000**, 4442–4445.
- (4) Adams, R. D.; Captain, B.; Pearl, W. C., Jr. *J. Organomet. Chem.* **2008**, *693*, 1636–1644.
- (5) Adams, R. D.; Hall, M. B.; Pearl, W. C., Jr.; Yang, X. *Inorg. Chem.* **2009**, *48*, 652–662.
- (6) (a) Cram, D. J.; Cram, J. M. *Science* **1974**, *183*, 803–809. (b) Gokel, G. W.; Leevy, W. M.; Weber, M. E. *Chem. Rev.* **2004**, *104*, 2723–2750. (c) Schneider, H. J. *Angew. Chem., Int. Ed. Engl.* **1991**, *30*, 1417–1436. (d) Lagona, J.; Mukhopadhyay, P.; Chakrabarti, S.; Isaacs, L. *Angew. Chem., Int. Ed.* **2005**, *44*, 4844–4870. (e) Lee, J. W.; Samal, S.; Selvapalam, N.; Kim, H.-J.; Kim, K. *Acc. Chem. Res.* **2003**, *36*, 621–630.
- (7) Crooks, R. M.; Zhao, M. Q.; Sun, L.; Chechik, V.; Yeung, L. K. *Acc. Chem. Res.* **2001**, *34*, 181–190.
- (8) (a) Leininger, S.; Olenyuk, B.; Stang, P. J. *Chem. Rev.* **2000**, *100*, 853–908. (b) Pluth, M. D.; Bergman, R. G.; Raymond, K. N. *Acc. Chem. Res.* **2009**, *42*, 1650–1659. (c) Fiedler, D.; Leung, D. H.; Bergman, R. G.; Raymond, K. N. *Acc. Chem. Res.* **2005**, *38*, 351–360. (d) McKinlay, R. M.; Cave, G. W. V.; Atwood, J. L. *Proc. Natl. Acad. Sci. U.S.A.* **2005**, *102*, 5944–5948. (e) Fujita, M.; Umamoto, K.; Yoshizawa, M.; Fujita, N.; Kusukawa, T.; Biradha, K. *Chem. Commun.* **2001**, 509–518. (f) Koblenz, T. S.; Wassenaar, J.; Reek, J. N. H. *Chem. Soc. Rev.* **2008**, *37*, 247–262.
- (9) (a) Conn, M. M.; Rebek, J. *Chem. Rev.* **1997**, *97*, 1647–1668. (b) Atwood, J. L.; Barbour, L. J.; Jerga, A. *Proc. Natl. Acad. Sci. U.S.A.* **2002**, *99*, 4837–4841.
- (10) (a) Houk, K. N.; Leach, A. G.; Kim, S. P.; Zhang, X. *Angew. Chem., Int. Ed.* **2003**, *42*, 4872–4897. (b) Hill, D. J.; Mio, M. J.; Prince, R. B.; Hughes, T. S.; Moore, J. S. *Chem. Rev.* **2001**, *101*, 3893–4012.
- (11) Adams, R. D.; Pearl, W. C., Jr.; Wong, Y.; Zhang, Q.; Hall, M. B.; Walensky, J. R. *J. Am. Chem. Soc.* **2011**, *133*, 12994–12997.
- (12) Raja, R.; Adams, R. D.; Blom, D. A.; Pearl, W. C.; Gianotti, E.; Thomas, J. M. *Langmuir* **2009**, *25*, 7200–7204.
- (13) Pearl Jr., W. C. Ph.D. Thesis, University of South Carolina, Columbia, SC, USA, 2010.
- (14) SAINT+ Version 6.2a; Bruker Analytical X-ray System, Inc.: Madison, WI, USA, 2001.
- (15) Sheldrick, G. M. *SHELXTL Version 6.1*; Bruker Analytical X-ray Systems, Inc.: Madison, WI, USA, 1997.
- (16) ADF2013; SCM Theoretical Chemistry, Vrije Universiteit: Amsterdam, 2013 (available via the Internet at <http://www.scm.com>).
- (17) Perdew, J. P.; Ruzsinszky, A.; Csonka, G. I.; Vydrov, O. A.; Scuseria, G. E. *Phys. Rev. Lett.* **2008**, *100*, 136406.
- (18) The numbers given in the figure caption are the observed numbers from the crystallographic analysis. Since this crystal contains 51% **6** and 49% **5**, the observed numbers are really an average of the distances in **5** and **6**. One can obtain a better estimate of the true distances in **5** by recalculating using an expression that accounts for the partial occupancy, e.g. $(0.49x + 0.51y = z)$, where x = the bond distance observed in **6**, z = the bond distance observed in this mixed crystal of **5** and **6**; y is the unknown and would be the bond distance expected for **5** in a crystal that contain 100% **5**. By using this calculation, the estimated interatomic distances (Å) in a crystal of pure **5** would be: $\text{Re}(1)-\text{Re}(2) = 3.5789(7)$, $\text{Re}(3)-\text{Re}(4) = 3.4538(6)$, $\text{Pd}(1)-\text{Re}(1) = 2.9348(18)$, $\text{Pd}(1)-\text{Re}(2) = 2.9455(19)$, $\text{Pd}(1)-\text{Re}(3) = 2.9820(18)$, $\text{Pd}(1)-\text{Re}(4) = 2.9823(19)$, $\text{Re}(1)-\text{Sb}(1) =$

2.7696(10), Re(2)–Sb(2) = 2.8012(10), Pd(1)–Sb(1) = 2.6306(18), Pd(1)–Sb(2) = 2.6351(18), Pd(1)–H(1) = 1.90(10), Pd(1)–H(2) = 1.76(10), Re(1)–H(1) = 1.82(10), Re(2)–H(1) = 1.68(10), Re(3)–H(2) = 2.07(9), Re(4)–H(2) = 1.84(10).

(19) Churchill, M. R.; Amoh, K. N.; Wasserman, H. J. *Inorg. Chem.* **1981**, *20*, 1609–1611.

(20) Mentès, A.; Kemmit, R. D. W.; Fawcett, J.; Russell, D. R. *J. Organomet. Chem.* **1997**, *528*, 59–63.

(21) (a) Adams, R. D.; Chen, M. *Organometallics* **2013**, *32*, 2416–2426. (b) Moret, M.-E.; Chen, P. *Organometallics* **2008**, *27*, 4903–4916. (c) Moret, M.-E.; Chen, P. *J. Am. Chem. Soc.* **2009**, *131*, 5675–5690. (d) Fernandez, E. J.; Laguna, A.; Lopez-de-Luzuriaga, J. M.; Monge, M.; Montiel, M.; Olmos, M. E.; Rodriguez-Castillo, M. *Organometallics* **2006**, *25*, 3639–3646. (e) Adams, R. D.; Captain, B.; Zhu, L. *Inorg. Chem.* **2007**, *46*, 4605–4611.

(22) Bau, R.; Drabnis, M. H. *Inorg. Chim. Acta* **1997**, *259*, 27–50. (b) Teller, R. G.; Bau, R. *Struct. Bonding (Berlin, Ger.)* **1981**, *41*, 1–82.

(23) Adams, R. D.; Captain, B.; Pearl, W. C., Jr. *J. Organomet. Chem.* **2010**, *695*, 937–940.